Pergamon

Cement and Concrete Research 30 (2000) 1869–1877

CEMENT AND CONCRETE RESEARCH

Impact of prolonged warm (85°C) moist cure on Portland cement paste

M. Paul, F.P. Glasser*

Department of Chemistry,University of Aberdeen 033 Meston Building, Meston Walk, Old Aberdeen, AB24 3UE Scotland, UK

Received 1 December 1999; accepted 13 April 2000

Abstract

A commercial Portland cement paste was fabricated as ~200-g cylinders to a water/cement weight ratio of 0.50. After ~30 days cure at ~20°C, cylinders were additionally cured at ~20°C and 85°C, both ± 2°C, in sealed, vapour-saturated systems for ~8.4 years. Thereafter, cylinders were allowed to stand, still in sealed state, at ~20° for 1.5 to 2.0 years. The 20°C cure mineralogy and microstructure is essentially normal: only a little unhydrated clinker persists and the matrix consists of relatively coarse, blocky $Ca(OH)_2$ crystals embedded in a groundmass of C-S-H together with some AFt (ettringite). However, prolonged 85°C cure significantly alters the microstructure and mineralogy. Clinker hydration progressed only slowly between 28 days and 8.4 years, with the result that ~30% cement clinker persists. Subsequent prolonged storage at ~20°C has apparently not allowed hydration to restart. $Ca(OH)_2$ is present in approximately unchanged amounts, comparing the two cures, provided allowance is made for the presence of unhydrated clinker. Paste porosity is, however, significantly increased at 85°C relative to ~20° cure. The 85°C mineralogy consists of four solid hydrate phases: $Ca(OH)_2$, C-S-H gel, with a Ca/Si mole ratio close to 1.52, katoite (a siliceous hydrogarnet) and a hydrotalcite-like phase. The amounts of these phases are determined. The compositions of the C-S-H gel and hydrogarnet have been estimated by transmission electron microscopy and microprobe analysis. The amount and composition of the mineral phases can be recalculated to yield a bulk composition of the cement that agrees with a batch analysis.

Keywords: Warm curing; Hydrogarnet; Paste mineralogy; Ageing; C-S-H

1. Introduction

Large masses of cement and concrete may experience a significant but transient thermal excursion during the early stages of hydration but prolonged exposure to temperatures in excess of 40°C is unusual except in a restricted range of environments: for example, in deep mines, in oil and geothermal wells and in radioactive waste repositories containing heat-generating wastes. Cement formulations may also be autoclaved, typically at 140–200°C, but experience shows that the bulk composition of cement must be altered by inclusion of much reactive silica to obtain a product with reasonable mechanical strength. Thus, comparatively little experience is reported in the literature of the long-term behaviour of unmodified, or slightly modified, Portland cements in moist environments in the temperature range 50–85°C.

In this paper we report on a unique set of samples. In 1989, a commercial Portland cement was cast into cylinders, ca. 42 mm diameter weighing ~200 g. Initially these were all moist cured for ~30 days at 20°C, but thereafter cylinders were moist cured, some at ~20°C and some at 85°C, for 1 and 8.4 years. The samples were finally removed from the test chamber in 1997 and stored, still in sealed containment, at ~20°C pending examination. We compare the mineralogy, microstructure, chemistry and porosity of these samples. Subsequent papers will extend these studies to compare and describe the thermally induced changes in fly ash and slag blends, after ~30 days normal curing, followed by 8.4 years at either 25°C or 85°C with additional subsequent ~20°C storage.

2. Previous studies

In a series of papers, Kjellsen et al. [1–4] report on the microstructure of cement pastes hydrated at different temperatures in the range between 5°C and 50°C. The back-scattered electron images of cement paste, (w/c = 0.5) hydrated at 50°C for 10 days to achieve 70% hydration, revealed four solid phases: unreacted cement clinker,

* Corresponding author. Tel.: +44-1224-27-29-06; fax: +44-1224-27-29-08.

0008-8846/00/$ – see front matter
PII: S0008-8846(00)00286-6

$Ca(OH)_2$, and two different forms of CSH, characterised by differences in optical density. Dense hydration shells, consisting of CSH and probably corresponding to inner hydrate, had formed around the unreacted cement grains. However, much of the matrix consisted of a lower density C-S-H, termed outer hydrate. The two CSH types had a sharp boundary. Although the morphologies of $Ca(OH)_2$ crystals and of the hydration shells were discussed and correlated with pore structure, no quantitative mineralogical data were given for the phases present.

Skalny and Odler [5] reported on the BET-surface area of synthetic C_3S pastes hydrated at 25°C, 50°C, 75°C and 100°C for 28 days. A decrease in surface area towards water vapour was observed with increase of curing temperature, but no explanation for the decrease was given.

Buck et al. [6] investigated the stability and persistence of ettringite and gypsum in cement and blended cements cured at 23°C, 50°C, 75°C and 100°C for up to 1 year by XRD and found that the ettringite content was reduced at 75°C and disappeared at 100°C except when additional Al, Ca, and S were available. Additional sources of Al, Ca, and S were obtained by blending the cement with fly ash. The additional supply of these species was believed to stabilise ettringite in the higher-temperature regime. When the content of ettringite did decrease, as occurred in prolonged cures at 100°C, it was not replaced, as expected, by monosulfate; instead hydrogarnet had formed.

In summary, the previous literature discloses limited information about the behaviour of cement during prolonged warm cure; most observations relate to relatively brief cure durations not exceeding 1 year. There is, however, evidence from these studies that cement clinker surviving initial cure can become very resistant to subsequent hydration at elevated temperature despite the continuing presence of free water.

3. Experimental

Cement cylinders approximately 42 mm diameter and weighing ~200 g were mixed to a w/c ratio of 0.5. The cement used was obtained from a commercial source in 1988/1989 and was made to British Standard 12. Its analysis, furnished by the manufacturer, is shown in Table 1: chemically and mineralogically it is close to an ASTM Type 1 cement. Neat paste cylinders were cast into "Perspex" moulds, covered top and bottom and turned end-on-end during initial set to avoid bleed and segregation. The high w/c ratio was deliberate, to ensure sufficient water for hydration. After ~24 h, the samples were de-moulded and heat sealed into plastic bags, to which had been added a few drops of water, using a commercial sealing device and allowed to cure for ~30 days at 20°C. After 30 days the samples were resealed into double layer thick-walled bags to which a few drops of water had been added. As a further precaution the doubled bags were placed in thick-walled autoclavable translucent plastic bottles to which a few ml of water had been added. The continuing presence of liquid water in the plastic bottles served as a visual check on the integrity of the seals. Once the water level began to fall within any one container, all samples on the same isotherm were re-packaged. In year 8, the schedule of container replacement could no longer be guaranteed so the warm-cure tests were discontinued in late 1997 after a cumulative 8.4 years at 85°C. The samples were kept sealed at ~20°C in moist CO_2-free conditions until they could be examined in 1998 and 1999.

Table 1
Composition of the Portland cement

Component	wt.%
SiO_2	20.50
Al_2O_3	4.91
Fe_2O_3	3.09
CaO	63.96
MgO	2.63
K_2O	0.57
Na_2O	0.07
SO_3	2.85
$\sum$	98.58

4. Results

4.1. Mineralogical development

Mineralogical development was determined by X-ray diffraction of bulk compositions and of selective dissolution residues, by microprobe analyses and by DTA/TGA. Analysis reveals that only minor carbonation, mainly affecting the near-surface layers, occurred during fabrication, packaging and storage. Consequently, all characterisation data were obtained from paste removed from the interior. The mineralogy of the 25°C cure was normal for a mature OPC: virtually all (≥98%) of the clinker had hydrated during cure and prolonged storage. The hydrated phases consisted of a low crystallinity calcium silicate hydrogel (shorthand, C-S-H), and three crystalline phases: $Ca(OH)_2$, ettringite (AFt), and AFm. The 85°C cure, on the other hand, gave a substantial amount of unhydrated clinker, the amount of which remained virtually unchanged between 28 days and 9–10 years, as well as four hydrate phases: C-S-H, $Ca(OH)_2$, hydrogarnet and hydrotalcite. The hydrotalcite-like phase gave only weak reflections and was best characterised from selective dissolution residues, in which it concentrated. The C-S-H at 85°C was slightly better crystallised than in 25°C cure but not sufficiently well crystallised for its X-ray powder patterns to resemble those of tobermorite or jennite. Ettringite and AFm phases were absent. As will be shown, the aluminate and sulfate formerly present in these phases has been redistributed onto sites in other cement phases.

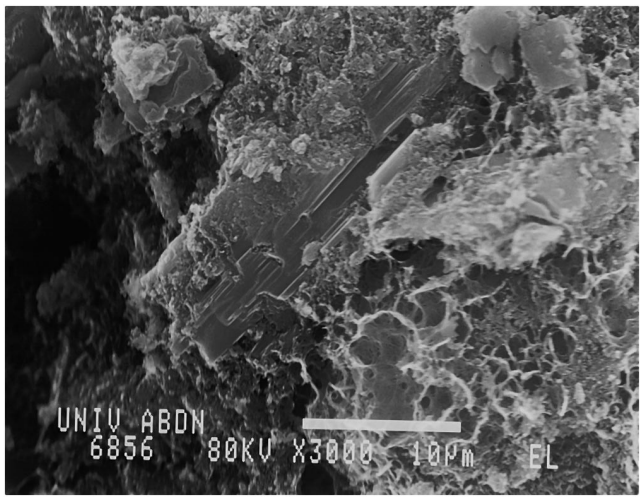

Fig. 1. Scanning electron micrograph showing the fracture of cement paste cured 30 days at 25°C, followed by 8.4 years at 85°C and, subsequently, ~1.5 years at ~20°C. Large $Ca(OH)_2$ crystals are visible towards the centre of the field of view: note their good cleavage. The porous matrix is a mixture of mainly hydrogarnet and C-S-H with numerous pores.

4.2. Mineral chemistry

The constituent phases, except for $Ca(OH)_2$, have a small and relatively even grain size, typically 1–2 μm in 85°C cures: Fig. 1 shows a scanning electron microscope image of the 85°C product. The large amount of unhydrated clinker is evident especially as it is surrounded by an envelope of dense, inner hydrate. $Ca(OH)_2$ occurs as 1–10 μm blocks and platey masses most readily visible in SEM of fractured surfaces in which its morphology, controlled by cleavage, is usually apparent.

The chemical compositions of the phases present have been analysed by TEM, equipped with an energy-dispersive analytical system and with a "Cameca" electron microprobe, equipped with a wavelength dispersive system, which could analyse several elements simultaneously. Much has been written about optimisation of the analysis of fine-grained cement materials by electron optical methods: briefly, it was found that correct choice of accelerating voltage, careful selection of grains and crystallites for analysis and frequent recalibration against appropriate standards is as important, or perhaps more important, than the choice of analytical system. With grain sizes typically only 1 to 2 μm in 85°C cures, TEM gave the best spatial resolution but its energy-dispersive analytical system required deconvolution of signal energies for Mg, Al, and Si with potential for error. As a consequence of the relative abundances of these elements and of the deconvolution procedures, large standard errors were frequently encountered for magnesium.

Some data arising from phase mixtures are also included. Where this is done, the procedures are explained and justified. Physical separation of hydrogarnet was also attempted using heavy liquids and centrifugation. However, hydrogarnet and unreacted clinker have similar densities, in the range 3.0 to 3.2 g/cm^3, and, as both were abundant in 85°C cures, the method was not successful in achieving physical separation.

4.3. Hydrogarnet

Table 2 records superior analyses obtained for hydrogarnet using TEM and microprobe. For reasons that are not entirely clear, the main interfering impurity in TEM arose from C-S-H contamination, whereas in EMPA it tended to be $Ca(OH)_2$. Supplementary analyses of $Ca(OH)_2$ were made: these data are not shown but disclose that the portlandite was chemically virtually pure and contained $\leq$ 1 mol% total of Mg, Al, Si, Fe, and S. However, all analyses of hydrogarnet reveal substantial contents of the expected elements, as well as of Si, Fe, Mg, and S. In order to recalculate the analyses to atomic populations the following scheme was used for grains believed to consist of hydrogarnet alone. The compositions of naturally occurring hydrogarnet, as well as of hydrogarnet encountered in synthetic studies, lie on the join $Ca_3(Al, Fe)_2 (SiO_4)_{3-x} (OH)_{4x}$: that is, two independent coupled substitutions occur, of (FeIII) for Al, and of SiO_4^{4-} for $4(OH^-)$. The trivalent ion substitution is straightforward isomorphous replacement. Stoichiometrically, the same is true for $SiO_4 \rightleftharpoons 4OH$ replacement, although the actual sites or set of sites occupied by the two tetrahedral

Table 2
Atomic population of hydrogarnet relative to 3.00 calcium

Al	Fe	Mg	Si	S	Si+S	*OH*
(A) Analyses made by TEM/EDAX						
1.583	0.317	0.101	2.477	0.383	2.860	*0.559*
1.695	0.211	0.940	2.058	6.523	2.518	*1.677*
1.573	0.299	0.128	1.232	0.368	1.600	*5.600*
1.698	0.209	0.093	1.179	0.274	1.453	*6.185*
1.687	0.199	0.115	1.104	0.264	1.368	*6.526*
1.671	0.180	0.149	2.124	0.283	1.407	*6.369*
1.629	0.251	0.120	1.180	0.275	1.455	*6.179*
1.531	0.270	0.200	1.010	0.282	1.292	*6.892*
1.292	0.637	0.071	1.512	0.301	1.813	*4.749*
1.630	0.178	0.192	1.189	0.246	1.435	*6.257*
(B) Analyses made by #EPMA/WDA						
1.572	*0.259*	*0.169*	*1.510*	*0.351*	*1.861*	4.555
0.883	*0.933*	*0.184*	*1.411*	*0.279*	*1.690*	5.240
1.186	*0.554*	*0.260*	*1.277*	*0.286*	*1.563*	5.749
1.302	0.425	0.272	1.361	0.279	1.640	5.440
1.246	0.649	0.105	1.696	0.300	1.996	4.016
1.142	0.723	0.135	1.544	0.302	1.846	4.613
1.134	0.732	0.135	1.549	0.286	1.835	4.659
1.043	0.743	0.214	1.319	0.299	1.548	5.810
1.581	*0.213*	*0.269*	*1.396*	*0.288*	*1.684*	5.262
1.403	*8.285*	*0.311*	*1.245*	*0.277*	*1.521*	5.918
1.405	0.229	0.366	1.237	0.280	1.517	5.932

Analyses in italics are believed to be effected by phases other than hydrogarnet and not used in subsequent calculations.

Abbreviations: TEM, transmission electron microscopy; EDAX, energy dispersive analyses for X-rays; EPMA, electron microprobe microanalysis; WDA, wavelength dispersive analyses.

substituents may differ. Apparent minor discontinuities in the solid solution series of silica-substituted hydrogarnets have been observed experimentally and recent structure determinations on naturally occurring hydrogarnets reported in Ref. [7] point to different tetrahedral site occupancies for SiO_4 and 4OH. Thus, we know the stochiometry of the substitution that enables water to be determined by difference, but not necessarily the substitution mechanism in terms of site occupancies. Fortunately, it is not necessary to know site occupancies with respect to Si and OH to interpret the analytical data.

Other problems of distribution occur concerning substitution of Mg and S in hydrogarnet. Several possible substitutions were considered for Mg: (i) that is substitutes for Ca, (ii) that it substitutes for Al in octahedral sites, (iii) that it substitutes for SiO_4 and/or 4OH in tetrahedral sites, and (iv) that it is distributed amongst more than one site. In naturally occurring hydrogarnets, only limited substitution of Mg occurs at high co-ordinate Ca sites except possibly at high pressures. Also, substitution of Mg into tetrahedral silicate sites is not observed at low pressures. Optimisation of cation populations amongst sites strongly suggests that all, or nearly all, the Mg must be in octahedral sites, so that structurally Mg can be included with Al and Fe. However, this substitution creates a charge imbalance of one positive charge per Mg but, as will be shown, this is compensated at least in part by other substitution mechanisms. Sulfur, as sulfate, is also reported as a substituent of naturally occurring hydrogarnet, for example in katoite, ideally $Ca_3Al_2(SiO_4)_{3-x}(OH)_{4x}$, in which sulfate has been assigned to tetrahedral sites [8]. This distribution of sulfate also provides the most acceptable reconciliation with the chemical analysis obtained in the course of the title study. But each $(SO_4)^{2-}$ group that substitutes produces a deficit of two negative charges on tetrahedral sites. However, depending on overall stoichiometry, this apparent deficit helps compensate, in whole or in part, for the deficit of positive charges occurring on octahedral sites as a consequence of introducing Mg. Thus, the preferred composition of the hydrogarnet has the ratios and site distributions given by the following incomplete formula: dots denote missing O, OH and H_2O.

$$Ca_{44.84}(Al_{18.88}Fe_{7.64}Mg_{3.37})(Si_{20.99}S_{4.28})\ldots\ldots$$

Attempts to determine water independently by TG (thermogravimetric) analysis were not successful. The TG step for water loss, which is usually well-resolved for C_3AH_6, tends to broaden and become diffuse for siliceous hydrogarnet solid solutions. Hence, water has been calculated by difference, to achieve electrostatic charge balance. Relative to Ca=3.00, the hydrogarnet formula therefore becomes:

$$Ca_3(Al_{1.26}Fe_{0.51}Mg_{0.23})[(SiO_4)_{1.40}(SO_4)_{0.29}(OH)_{5.59}]$$

This method of balancing produces 11.77 positive and 11.77 negative changes and may be compared with a theoretical value of 12.0 for either hydrogarnet, C_3AH_6, or grossularite. The population ratio of Ca to the sum on octahedral sites is exactly 1.50, i.e., the theoretical value.

The unit cell content of this hydrogarnet, calculated from least squares refinement of its powder data, has $V = 1888$ Å^3 (± 2 Å^3). The calculated density is 3.14 g/cm^3, rounded to 3.1 g/cm^3 for subsequent calculations.

Analyses believed to arise from $Ca(OH)_2$–hydrogarnet mixtures were plotted on a ternary diagram having as apices $Ca(OH)_2$, $\sum$ octahedral substituents and $\sum$ tetrahedral substituents. Since $Ca(OH)_2$ is known to be essentially free of substituents, the analyses points of $Ca(OH)_2$–hydrogarnet mixtures should lie on a tie line connecting the $Ca(OH)_2$ composition with that of the hydrogarnet, as deduced above. This condition was met and the presence of $Ca(OH)_2$ confirmed in selected, high-calcium examples by selected area electron diffraction. A similar procedure was used to resolve mixtures of hydrogarnet with C-S-H. The accuracy of fit was less good because the plot discloses that $Ca(OH)_2$ was in all probability also present and because of the more complex chemistry of C-S-H and associated analytical uncertainties, see below.

4.4. Calcium silicate hydrate, C-S-H

The non-crystalline nature of C-S-H removes some of the restraints on its composition that tend to restrict substitution in a crystalline phase. Table 3 shows the results of analyses made by both TEM with EDAX detection and

Table 3
Normalised atomic ratios in C-S-H

Ca	Al	Fe	Mg	Si	S
(A) Analyses made by TEM/EDAX					
61.16	1.38	0.37	0.77	30.84	4.51
59.69	−2.05	0.13	−0.75	39.00	2.94
58.60	−2.00	0.38	−0.34	39.43	2.94
57.62	−1.97	0.30	1.59	38.90	2.70
56.69	0.48	0.37	3.63	36.33	1.65
58.09	−2.68	0.43	−0.49	38.04	6.06
60.49	−0.95	1.16	0.23	34.71	3.90
63.86	−4.19	0.71	00.40	35.88	3.23
61.38	−0.48	0.35	0.15	34.97	3.12
59.82	−0.32	0.36	−0.09	36.84	2.63
(B) Analyses made by EPMA/WDA					
56.84	0.71	0.44	0.42	38.58	3.01
57.66	0.68	0.00	1.73	36.59	3.34
57.53	1.19	0.29	2.64	35.33	3.03
55.60	0.69	0.96	1.67	37.70	3.38
55.93	0.88	0.59	1.98	37.47	3.15
55.37	0.91	1.27	2.01	37.25	3.21
057.10	0.64	0.88	0.69	37.42	3.28
56.59	0.54	0.88	0.66	37.46	3.86
56.58	0.78	0.66	1.49	37.21	3.28
(0.18)	(1.16)	(0.33)	(0.65)	(0.64)	(0.18)

Abbreviatons: TEM, transmission electron microscopy; EDAX, energy dispersive analyses for X-rays; EPMA, electron microprobe microanalysis; WDA, wavelength dispersive analyses.

EPMA with wavelength dispersion. On balance, we feel that the EPMA results obtained at 5 kV acceleration potential comprise the most reliable dataset. Accordingly, mean values and standard deviations are given for this set. The mean formula of the calcium silicate, excluding water, in the 8.4-year cure at 85°C is:

$$Ca_{56.58}Al_{0.78}Fe_{0.66}Mg_{1.48}Si_{37.21}S_{3.28}\ldots\ldots$$

Its mean Ca/Si ratio is thus 1.52; this compares with a mean ratio of 1.72 ± 0.05 obtained from analyses on C-S-H cured at 25°C. Rather little substitution by Al and Fe occurs in the 85°C cures; that which is observed is presumably mainly on tetrahedral sites. However, if these substituents are included amongst the tetrahedral site population the atomic ratio of Ca: (Si + Al + Fe + Mg) decreases to 1.41. The structural role of sulfate is uncertain: provisionally, it is allocated in place of OH^-. But, since we were not successful in deconvoluting the TGA, and hence in obtaining an independent measure of bound water, the analysis remains incomplete. However, for mass balance calculations, we need to assign a water content and for this purpose note that normal C-S-H, made at Ca: Si∼1.7 and at 25°C, has a water content represented by the formula 1.7 $CaO{\cdot}SiO_2{\cdot}1.3-1.5\ H_2O$ [10]. The water contents of some low Ca/Si ratios have also been determined independently in our laboratories and lie within this range, probably closer to the limits 1.3 to 1.4 than to 1.5. Thus, a working formula for C-S-H developed at 85°C is:

$$CaO_{56.58}[(SiO_2)_{37.21}(AlO_{1.5})_{0.78}(FeO_{1.5})_{0.66}(MgO)_{1.48}]_{40.13}\ [(SO_3)_{3.78}(H_2O)_{52}]_{55.28}.$$

4.5. Hydrotalcite-like phases

Insufficient hydrotalcite was obtained to permit a satisfactory direct analysis by microprobe or TEM. The chemically determined ratio of Mg/Al+Fe in selective dissolution residues was ∼3.0. However, the dissolution residues were known to consist of mixtures of phases, so the ideal ratio of divalent to trivalent ions, 3.0, was assumed in subsequent calculations. Possible errors arising from this procedure are discussed subsequently.

4.6. Mass balances

Preliminary calculations of mass balances were made as follows. The presence of much clinker in the 85°C cure made it necessary to determine the amount of unreacted clinker present. This was done by point counting of a polished thin section using an optical microscope. Five thousand grid points were counted and the amount of unhydrated clinker, assuming its mean density to be ∼3.1 g/cm^3, was found to be 30.1 ± 1 wt.%. It was also necessary in subsequent steps to assume that the mean atomic ratios of the hydrated paste were the same as in the clinker, except of course for water. This problem of the persistence of clinker does not arise at 25°C, where hydration is virtually complete, but is potentially a problem at 85°C; if selective hydration of clinker components were to occur the paste might become enriched in some components and correspondingly depleted in others. Accordingly, we inspected the margins of clinker grains by EMPA for signs that one or more clinker phases were being selectively hydrated. No evidence was found that selective or differential hydration occurred: for example, that alite hydrated faster than belite, or that alite and belite hydrated preferentially to interstitial material. The hydration of clinker seemed to follow a regular course, preserving a sharp interface with paste, free from embayments and we therefore assume mean atomic ratios in the paste to be the same as in clinker, water and sulfate excepted.

In order to calculate the remaining mass balances, it was essential to determine the phase percentages of each mineral. The quantities of the phases present were determined as follows. The clinker content was known from point counting. $Ca(OH)_2$ was determined by the modified Franke extraction method as well as by TGA. In the Franke method, $Ca(OH)_2$ was selectively extracted into an acetoacetic ester-2 methyl propanol solvent, using a reflux apparatus. The filtered solution was titrated with standard perchloric acid in isobutanol, using thymol blue as an indicator. The cement cured at 85°C gave 19.0 wt.% $Ca(OH)_2$ while the 25°C cure gave 24.9 wt.%; TGA gave essentially the same results: 19.0% (85°C cure) and 25.4% (25°C cure). The amount of $Ca(OH)_2$ is apparently reduced in 85°C cures relative to 25°C, but it should be recalled that considerable unhydrated clinker, with potential to form more $Ca(OH)_2$, persists in the paste cured at 85°C.

The amount of hydrotalcite present could not be determined reliably from the weight of dissolution residues, as they were not phase pure. Moreover they could not be completely dried to constant weight as this would have destroyed the fragile hydrotalcite. Rough gravimetric estimates of the mass of hydrotalcite-containing residues, together with an estimate of purity, suggested that the hydrotalcite content of the bulk paste was on the order of 2%. However, it is apparent that the maximum amount of hydrotalcite must be limited by the total Mg present, bearing in mind that not all magnesium in the paste is available for hydrotalcite formation, some being fractionated into hydrogarnet and C-S-H. Trial-and-error calculations based on magnesium distributions suggested that a reasonable estimate of the hydrotalcite content was 1.5 wt.% and this value was used in subsequent calculations. Since the absolute numerical value of the hydrotalcite content is low, subsequent calculations disclosed that the overall phase balance was not particularly sensitive to changes in the amount of hydrotalcite in the range 1–2%.

Hydrogarnet was estimated by quantitative X-ray diffraction, using weighted mixtures of $Ca(OH)_2$ and hydrogarnet for calibration. Because we did not have a synthetic hydrogarnet of precisely the right composition and, indeed, did not know its composition at the outset, synthetic C_3AH_6

was used as a standard. The X-ray intensities and positions of diffraction maxima reported in the powder diffraction file for C_3AH_6 [9] are essentially identical with those of a silica-substituted hydrogarnet, suggesting that this procedure, while not ideal, is at least satisfactory. In practice the standard deviation of the method was not as good as we hoped for and the content of hydrogarnet in the 85°C cure sample was estimated by quantitative X-ray diffraction to lie within the range 16–25%.

Because of the large uncertainties in estimating hydrogarnet, the remaining phases were estimated by constructing a table of mass balances, first subtracting clinker, $Ca(OH)_2$ and hydrotalcite, and subsequently optimising the remaining balances, introducing as appropriate additional evidence based on patterns of element distribution. For example, most of the Al not already assigned to hydrotalcite occurred in hydrogarnet, not C-S-H, and the maximum amount of hydrogarnet must be essentially limited by the population of unassigned Al. A sensitivity study was also made to determine if arbitrary changes to the amounts of hydrogarnet and C-S-H affected the results. In fact, the calculated balances were already close to optimum. The final mineralogical balances are 30% clinker, 20–21% $Ca(OH)_2$, 1.5% hydrotalcite, 16% hydrogarnet and 31.5–32.5% C-S-H: Table 4 gives optimised values used in subsequent calculations. These mineral balances, taking the analytically determined formulae into account, were used to recalculate the bulk composition and account for ~96 mass% of the total substance of the anhydrous cement.

4.7. Porosity

Fig. 2 records the mercury intrusion porosimeter data obtained on otherwise identical samples (top) continuously cured for ~10 years at 20°C and (bottom) for 8.4 years at 85°C followed by ~2 years at 20°C. At the maximum pressure attainable, *ca* 2000 bars, the intrudible volume is ~0.1 cm^3/g paste following 20°C cure. A slight but characteristic inflection occurs at a pore entry diameter in the range 0.05–0.06 μm. In contrast, following 85°C cure, the accessible volume is greatly increased, to ~0.23 cm^3/g. A very sharp inflection in the intruded volume–pore entry diameter curve occurs at above 0.1 μm. This marked increase is also visually evident from the backscattered electron images but because their resolution is only on the order of 0.05–0.1 μm, porosity cannot readily be quantified from the images. The very large increase in porosity following 85°C cure arises partly as a consequence of conversion of low-density paste constituents to higher-density hydrogarnet and partly because of the failure of much of the clinker to hydrate.

Table 4
Mass balances
Composition of paste cured 8.4 years at 85°C[a]

Mineral phase(s)	wt.%
Clinker	30.0
$Ca(OH)_2$	21.0
Hydrogarnet	16.0
C-S-H	31.5
Hydrotalcite	1.5

[a] Previous to 85°C, 1 month at ~25°C and subsequent to 85°C cure, 1.5 years at ~20°C.

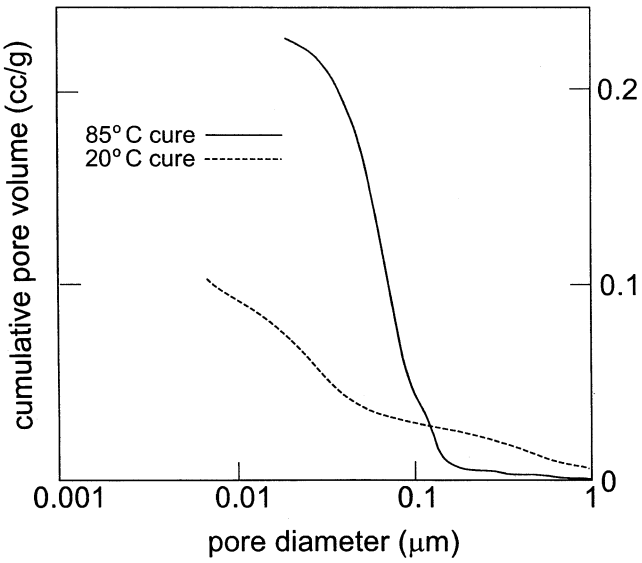

Fig. 2. Mercury intrusion porosity of OPC cured continuously at 20–25°C for ~10 years and cement initially cured for ~30 days at 25°C but subsequently for 8.4 years at 85°C followed by 1.5 years at ~20°C.

5. Discussion

It is apparent that the results obtained at 25°C illustrate the persistent nature of the early hydration products of Portland cement. It would be difficult convincingly to point to changes that we have identified as occurring between 1 and 10 years of hydration except that the small amount of clinker present after 1 year has diminished virtually to zero. However, further hydration beyond ~28 days at 25°C is very much a secondary process and does not much affect the hydrate phase distribution or the matrix microstructure, which continues to reflect features that were developed mainly within the first few hours or weeks of hydration. For example, relatively coarse $Ca(OH)_2$ crystals or crystal aggregates, developed early in the hydration process, persist. They are embedded in a fine-grained matrix of C-S-H, AFt and AFm, the microstructure of which remains essentially unchanged.

On the other hand, prolonged treatment at 85°C has inhibited hydration of residual clinker but significantly altered the mineralogy of the already-formed paste matrix. Clinker has persisted such that the 30-day distribution of clinker and hydrated paste has changed little after 8.4 years at 85°C and hydration has not renewed during a further 1–2 years at ~20°C. We first considered that, despite all pre-

cautions, the specimens must have desiccated leading to loss of water necessary to continue hydration. But analyses confirmed that the pastes still contain the expected content of evaporable water, i.e. water lost at <110°C. Despite ~2 years additional post-cure storage at ≥98% relative humidity and ~20°C, no evidence for ongoing bulk hydration in the post-cure phase was obtained. Moreover, previous relevant studies of curing at elevated temperature have also remarked on the persistence of unexpectedly large amounts of clinker. Whilst the experimental conditions (time, temperature, w/c ratios) of these previous studies are not directly comparable with those of the present study, the persistence of clinker in elevated temperature cures is a noteworthy and unexpected feature. If it is accepted that sufficient water persists to permit hydration, the remaining clinker must be protected against hydration in some way. One hypothesis is that the dense layer of inner hydrate which forms around residual clinker grains acts as a barrier to water transport. This layer is seen in backscattered electron images as a coherent, rather featureless but dense zone, a few micrometers thick in cross-section. Whereas normal C-S-H is sufficiently permeable to permit water to diffuse and sustain ongoing hydration of clinker, the inner hydrate layers formed in 85°C cures must, in this explanation, be effectively impermeable.

However, it seems improbable that layers of a nanoporous material could be sufficiently impermeable to result in a cessation, or virtual cessation, of hydration. C-S-H gels are characterised by their content of gel porosity and, ordinarily, a strong driving force exists for water vapour transport leading to condensation into capillary porosity. Thus, water should still be transported towards the clinker, albeit slowly. It is suggested that a series of processes operate to inhibit transport. Firstly, the cement grains develop a relatively dense layer of inner hydrate that slows but does not prevent access of water. However, as this layer thickens, a moisture gradient develops such that capillaries close to the cement clinker become partially dewatered. At the same time, rising temperatures also lead to degassing of pore fluid because the solubility of most common gases in water decreases with rising temperature. As water is removed by ongoing hydration at or near the margins of clinker grains, it is suggested that the capillary porosity becomes gas-filled. This gas is effectively pressurised by driving forces for capillary condensation. Eventually, a situation is reached such that the two pressures balance, with the result that water transport ceases and, as a consequence, clinker hydration stops. Although this scenario is incapable of direct proof from present evidence, it does resolve the apparent paradox that clinker particles persist at warm temperatures in a hydrous environment, protected only by a barrier that, in the absence of special circumstances, is nanoporous and, intrinsically, somewhat permeable to water.

Mass transport continues to occur in the bulk of the paste, with the result that its mineralogy and, in part, its microstructure are reconstituted. The main features of this reconstitution are four fold: (i) some phases, present at both 25°C at 85°C, change significantly in composition, for example C-S-H, (ii) other phases form at 85°C which are not normally developed at 25°C, hydrogarnet is an example, (iii) phases, probably present as amorphous material at 25°C, crystallise at 85°C (hydrotalcite); and finally, (iv) phases which are persistent at 25°C but which disappear at 85°C (AFt, AFm). The only constant constituent seems to be portlandite, $Ca(OH)_2$, which is present at both temperatures.

The C-S-H composition is markedly affected: at 85°C its mean Ca/Si ratio decreases to 1.52, less if other substituents believed to be in tetrahedral sites are added to silica. This relatively low ratio C-S-H appears to coexist with $Ca(OH)_2$. This contrasts with 25°C cures, in which only a high ratio C-S-H, with Ca/Si ~1.72, coexists with $Ca(OH)_2$.

The extent to which the phase distribution at 85°C is relevant to 25°C is speculative, but it is interesting to note that high Ca/Si ratios, >1.5, widely encountered in cement pastes hydrated at ~25°C are often explained by a two-phase structural model in which one phase consists of microcrystalline or amorphous "$Ca(OH)_2$" distributed in a lower-ratio C-S-H, the latter perhaps having a jennite or tobermorite-like structure. This and similar fictive models are often invoked to relate structure composition and solubility in the C-S-H family. The present results do not provide unequivocal evidence of C-S-H structure but they do indicate that high ratio ~C-S-H which forms and apparently persists at 25°C is rather unstable at elevated temperatures, converting to a lower ratio (1.52, if only Ca and Si are reckoned) C-S-H. This decreasing ratio effectively liberates calcium which is incorporated in other phases, mainly hydrogarnet. While evidence on the persistent compositional range at 85°C is not necessarily applicable to 25°C, structural models of C-S-H treating high ratio C-S-H as a solid solution may have some basis in reality: certainty prolonged annealing at 85°C discharges Ca from C-S-H in excess of Ca/Si ≥ 1.5, approximately.

The development of traces of hydrogarnet in warm-cured Portland cement product is well known. But the quantitative extent to which the reaction will proceed, given time, has not hitherto been documented. In the absence of specific information, the potential for hydrogarnet formation in normal Portland cements has always been considered to be limited by (i) the relatively low alumina content of Portland cements, relative to more aluminous types, e.g., high-alumina cement (ii) the persistence at ~25°C of ferrite, which retains significant alumina in comparatively inert form and (iii) competition for alumina by other space-filling hydrates, such as low density AFt and AFm phases. At 85°C many of these restraints are removed. Firstly, ferrite phase not present in unreacted clinker reacts and thus contributes calcium, alumina and iron to the chemical and mineralogical evolution of the paste. Of the ~70% of clinker which has hydrated at 85°C all, or virtually all, of its content of Al, and Fe, has entered into the constitution of

the hydrated paste. Secondly, aluminate phases persistent at 25°C cure do not occur at 85°C. Thus alumina, present at 25°C in AFt and/or AFm, is instead incorporated into other phases, notably hydrogarnet. Thirdly, alumina in octahedral sites is partly substituted by and hence extended by other ions: Fe and, in part, Mg. The generally low activity of silica in Portland cement is thus not a thermodynamic barrier to the formation of siliceous hydrogarnet, which appears to be a favoured phase at 85°C.

The time required for hydrogarnet crystallisation is noteworthy. When these cements were examined after 1 year cure at 85°C, only traces of hydrogarnet were detected: clearly, nucleation had occurred. No attempt was made to quantify the amount of hydrogarnet present at 1 year but the findings were roughly in accord with those reported in [6]. However, by 8 years at 85°C, the quantity of hydrogarnet had greatly increased, to *ca* 16%. We therefore conclude that nucleation of hydrogarnet in OPC compositions at 85°C requires on the order of a few hours to 1 year, while its crystallisation requires on the order of 10 years. This, in turn, raises three interesting questions: firstly, have we reached the end of the mineralogical changes at 85°C? Secondly, would the same sequence of events occurring at 85°C also occur at lower temperatures, albeit over longer periods of time? Finally, do experiments described in this paper have any lessons concerning much more brief thermal excursions?

With respect to the first question, the answer is almost certainly, no. The persistence of an amorphous, or nearly so, calcium silicate hydrate is a certain indicator of metastability. The gel-like phase is always thermodynamically metastable with respect to crystalline calcium silicate hydrates and, on that account, the paste may have attained a steady state, but if so its steady state cannot be an equilibrium. Nevertheless, the gel phase has obviously participated in reaction: its mean Ca/Si ratio diminished significantly and an extensive partition of minor elements (S, Al, Fe, etc.) occurred between gel and crystalline phases such that gel continues to coexist with hydrogarnet and a hydrotalcite-like phase. To reach a true equilibrium, C-S-H gel must crystallise, thus affording opportunity for another repartition of atomic species amongst phases, a process that will inevitably affect both nature and amount of phases present. We can, however, conclude that the assemblage of four solid phases—C-S-H, hydrogarnet, $Ca(OH)_2$ and a hydrotalcite-like phase—is persistent at 85°C.

Finally, the consequences of relatively brief thermal cycling have attracted much recent attention that has centred on ettringite. One characteristic of immature pastes is that, on being cycled to elevated temperatures, typically 60–90°C, the amount of AFt phase is much reduced, perhaps to zero. Yet, upon return to lower service temperatures ettringite reappears. This process, under circumstances as yet not fully defined, is expansive. In the samples annealed for much longer, 8.4 years at 85°C, AFt has also disappeared: sulfate is incorporated into other phases, notably into hydrogarnet and C-S-H. These samples have now had ~2 years post-heat treatment at ~20°C and 100% humidity but have yet to expand or crack. The significance of this observation is unclear: it may be simply that the cement used is an example of an intrinsically non-expansive material. But it may equally be that the two processes are not comparable: for example, short thermal cycles develop insufficient amounts of hydrogarnet to act as a significant storage system for sulfate. In this view, reformation of ettringite is inhibited by formation of sulfate-containing hydrogarnet.

With respect to the possible formation of a $Ca(OH)_2$–hydrogarnet–CSH–hydrotalcite assemblage at 25°C, analogous to 85°C, we can only speculate. A possible analogy might lie in high alumina cements, which should in theory develop hydrogarnet as a stable phase at all temperatures > 0°C. This process, termed 'conversion', occurs at a rate which is sharply temperature dependent but for practical purposes requires only a few years in moist conditions at temperatures as low as 30–40°C. We suggest a similar conversion is energetically feasible in Portland cement but that it is not observed to occur in moist warm service temperatures for kinetic reasons; reaction is too slow.

In aluminous cements, conversion is associated with a marked diminution of the physical volume occupied by paste constituents. Since the conversion is not marked by a shrinkage in geometric volume, much additional internal pore space is created. The same effect of increased internal pore space is noted from MIP scans of Portland cement, comparing 25°C and 85°C cures. In high alumina cements, conversion with increase in porosity results in a large decrease in strength. Owing to the insufficient number of samples, we have been unable to verify if strength regression occurs in Portland cement but suspect that the strength of the 85°C cure samples will have decreased both on account of (i) the relatively high content of unconsumed clinker and (ii) the relatively porous nature of the hydrated portion of paste.

Acknowledgments

The samples were initially laid down by grants from the UK Department of the Environment, now The Environment Agency for England and Wales, and the Commission of the European Communities. The post cure examination was supported by the Commission of the European Communities, contact F14W CT96 0030.

References

[1] K.O. Kjellsen, R.J. Detwiler, O.E. Gjørv, Backscattered electron imaging of cement pastes hydrated at different temperatures, Cem Concr Res 20 (1990) 308–311.
[2] K.O. Kjellsen, R.J. Detwiler, O.E. Gjørv, Pore structure of plain ce-

ment pastes hydrated at different temperatures, Cem Concr Res 20 (1990) 927–933.
[3] K.O. Kjellsen, R.J. Detwiler, O.E. Gjørv, Development of microstructures in plain cement pastes hydrated at different temperatures, Cem Concr Res 21 (1991) 179–189.
[4] K.O. Kjellsen, R.J. Detwiler, O.E. Gjørv, Backscattered electron imaging of cement paste specimens: specimen preparation and analytical methods, Cem Concr Res 21 (1991) 388–390.
[5] J. Skalny, I. Odler, Pore structure of calcium silicate hydrates, Cem Concr Res 2 (1972) 387–400.
[6] A.D. Buck, J.P. Burkes, T.S. Poole, Thermal stability of certain hydrated phases in systems made using Portland cement, Miscellaneous Paper Sl-84-7, US Department of Energy, Columbus, OH, 1975.
[7] T.G. Jappy, F.P. Glasser, Synthesis and stability of silica-substituted hydrogarnet, $Ca_3Al_2Si_{3-x}O_{13-4x}(OH)_{4x}$, Adv Cem Res 4 (1) (1991) 1–8.
[8] R.V. Ganes, H.C.W. Skinner, E.E. Foord, B. Mason, A. Rosenzweig, Dana's New Mineralogy, 8th edn.,Wiley, New York, 1997, p. 1052.
[9] The Powder Diffraction File, card 24-217 International Centre for Diffraction Data, Newton Sq., PA, USA, 1994.
[10] H.F.W. Taylor, Cement Chemistry, Academic Press, London and New York, 1992.